Impact of Surface Roughness on the Self-Assembling of Molecular Films onto Gold Electrodes for Label-Free Biosensing Applications

Gorachand Dutta[1,a], Flavio C. B. Fernandes[2], Pedro Estrela[1], Despina Moschou[1,#], Paulo R. Bueno[2,*]

[1]Centre for Biosensors, Bioelectronics and Biodevices (C3Bio) and Department of Electronic and Electrical Engineering, University of Bath, Bath BA2 7AY, UK
[2]Institute of Chemistry, São Paulo State University (UNESP), Araraquara, São Paulo, Brazil

Corresponding authors: [#]d.moschou@bath.ac.uk; *paulo-roberto.bueno@unesp.br

[a]Current address: School of Medical Science and Technology, Indian Institute of Technology Kharagpur, West Bengal-721302, India

Abstract

The properties of molecular films assembled over gold electrode surfaces are prone to reflect fabrication characteristics. Here we show the importance of controlling electrode surface characteristics of a gold interface destined to label-free electrochemical biosensing applications and how to decrease the effect of the roughness on the properties of the interface by using redox composite materials within 5 to 10 nm in thickness. This controlling of surface characteristics allows us to fabricate reproducible, disposable printed circuit board microelectrodes for label-free electrochemical capacitive assays, which are specifically aimed at applications in point-of-care molecular diagnostic devices. We demonstrate that both the electrochemical roughness factor and the mechanical roughness root mean square of the surface are useful parameters for the quality control of molecularly assembled films and the chemical modification of the surface. For instance, the measured ionic capacitance of gold interfaces is linear as a function of an electrochemical roughness factor lower than ca. 2. On the other hand, roughness factor values higher than ca. 2 lead to a random ionic capacitance outcome. A similar trend of presenting reproducible or irreproducible electrochemical behaviour, wherein a roughness threshold exists, is perceived for charge transfer resistance whether the interfacial redox activity is blocked with a dielectric molecular layer. It was also demonstrated that redox reversibility of gold interfaces is sensitive to the roughness root mean square. Finally, we also confirmed that if the roughness is controlled below a well-defined threshold or if a film thickness (within 5 to 10 nm) is assembled over the surface, the sensing properties are reproducible in micro-fabricated printed circuit board electrodes used in assaying C-reactive protein in human serum. This is an important upshot that permit the microfabrication of cost-effective microelectrodes for label-free electrochemical capacitive biosensors, within the capability to be further integrated into Lab-on-PCB microsystems.

Keywords: surface roughness, electrode surface characteristics, self-assembled monolayers, electrochemical biosensors, Lab-on-PCB

Introduction

The age of sensing technology is upon us[1] and this is evidenced by observing how we, consumers, are experiencing the rise of electronic products that apply different types of sensors. Sensors permit new ways for individuals to interact with portable, autonomous and home-based devices, ultimately bringing some pleasing experiences of how easy is to access the functionalities of a portable or home-based miniaturized hardware[2-5]. Nonetheless, developments toward miniaturization still have great limitations and challenges to be faced. For instance, though the use of molecular devices has been dreamt[6, 7] at the single molecular level and the single-molecule transistor paradigms have provided some fascinating scientific insights, there are still significant problems to integrate molecular transistors into valuable electronic devices. These challenges prevent the immediate usefulness of this approach, especially for applications requiring sensing at the biological environment.

Fortunately, there are other alternatives to the use of single molecule devices[8] and this is the case of using molecular films[3, 9-13]. Molecular films still keep the advantages of molecular scale approaches for sensing purposes if one of their dimensions, thickness for instance, are at the "nanoscale" within quantized charge storage and transport mechanism characteristics as described elsewhere[14, 15]. This ''nanoscale" quantized characteristic is referred as mesoscopic properties[8] and can be successfully designed in molecular films *if surface roughness or its effects on the mesoscopic properties are controlled*, for instance.

The fabrication of molecular films requires to preserve the quality of the collectiveness of the ensemble of molecules that are self-assembled and molecularly well-ordered over a solid-state conductive surface[14, 16]. These ensemble junctions contain a large number of molecules that are oriented in parallel between one (electrochemistry) or two (electronic) conductors and that can be, in terms of its surface, as large as 0.0025 cm^2, containing ca. 10^{12} molecules[14, 16-18] per cm^2. Obviously, a ca. 1 nm thick molecular layer assembled on a surface within >1 nm roughness is prone to defects that are able to cause significant variability on its mesoscopic[14, 17] properties. This is the case, for instance, of capacitive electro-active properties of molecular films[19] and specifically, by mesoscopic[14, 17] we are referring to those properties that are intermediate between the classical and quantum mechanics, where both quantum and classical contributions are indistinguishable and this is the case of the electrochemical capacitive properties of molecular films. To keep the capacitive properties reproducible special methods and protocols for controlling the properties of the surface are required[14].

The use of molecular self-organized ensemble approach has been used for several practical and fundamental reasons[14, 16-18], but the most important of them are that researchers knew how to make modified solid electrodes with molecules and could characterize them using both electronic and electrochemical methods[20-23]. The latter is quite useful specially for label-free biosensor applications, where modifications of the surface of the electrode with molecular moieties are made with the specific purpose of fabricating electrochemical sensing interfaces aiming at to the diagnosis of clinically important diseases[24-29] by detecting biological markers.

The present work deals with a specific fabrication problem which involves the assembly of molecular moieties onto conductive electrodes through an appropriate control of surface roughness[30-37]. We also demonstrate that limitations of fabricating reproducible surface roughness can be overcome by using redox composites within a thickness lower than 10 nm, thus assuring the reliability and reproducibility of biosensing interface, one of the most critical and often overlooked aspects of point-of-care (PoC) biosensor technologies[38]. Though a fundamental

fabrication problem, the roughness of electrode's surface is frequently disregarded in the literature. The ability of assembling molecular moieties onto conductive electrodes defines the success of the electronic and/or the electrochemical properties[39, 40] of the interface.

Within above context, the present work has the purpose of demonstrating how it is possible to achieve required surface features wherein the issue of roughness can be overcome, enabling molecular films to be assembled with indispensable reproducible characteristics and ultimately producing stable films for label-free electrochemical biosensors. Specifically, we provide indications and additionally we demonstrate how the required characteristics of a gold-disk electrode can be translated to a microfabricated gold-PCB (printed circuit board) interface. PCB electrodes enable the miniaturization of molecular assays onto disposable packages that can be potentially fabricated in a label-free biosensing[41] format, along with their subsequent integration into a complete Lab-on-PCB diagnostic microsystems[42] is possible. Therefore, the translation of the critical characteristics of a macro-electrode to a micro-fabricated interface is obviously of great commercial interest because it allows us rapidly to translate laboratory assays in a commercially viable format, permitting a quicker conversion of diagnostic assays from academic laboratorial space to a field-based PoC environment at a lower cost[43].

Methods of measuring surface roughness

There are different ways of defining and consequently of inferring (or of measuring) surface roughness. From an engineering metrological point of view, the roughness of a surface is defined as a component of the surface texture which can be quantified by deviations in the direction of the normal vector of a tangible surface from its ideal form, being the surface rough or smooth quantification dependent on the degree of deviation of the normal vector with respect to its ideal format. Because the normal vector is defined geometrically, the engineering denotation of surface roughness is, strictly speaking, a mathematical and spatial definition which is normally inferred statistically as[44]

$$R_q = \sqrt{\frac{1}{n}\sum_{i=1}^{n} {y_i}^2}, \quad (1)$$

which is known as root mean square of measured microscopic peaks and valleys of the surface and where the profile contains n ordered, equally spaced points along the trace, and y_i is the vertical distance perpendicular to the surface from the mean line to the ith data point. Surface roughness is not only a good predictor of the mechanical performance of a surface[45], but it also correlates with the chemical reactivity of the material's surface that controls corrosion and catalytic activities beyond other properties.

In the latter case, where surface roughness is associated to the chemical properties of the surface, one important admeasurement is the specific surface area which essentially provides an indirect way of measuring the surface's roughness of a chemical compound. The higher the specific surface the higher the exposition of the chemical "reagents" to the reactants, i.e. the greater the surface area the higher the expected reactivity. In electrochemistry, the specific surface area is commonly correlated, for instance, with electro-catalytic and capacitive characteristics of compounds and materials that are applied in catalysis and super-capacitor applications. Therefore, in electrochemistry, there is still another method of measuring surface roughness, i.e. by using the electrochemical roughness factor[31, 46] of the surface, δ. Essentially, the roughness factor is useful

because it is a good estimative of how electrons perceive the electrochemical reactivity and characteristics of an interface when it is immersed into an electrolyte. δ values are measured as the ratio between the electro-active area (A_e) and the geometrical area (A_g) of a working electrode[17, 36].

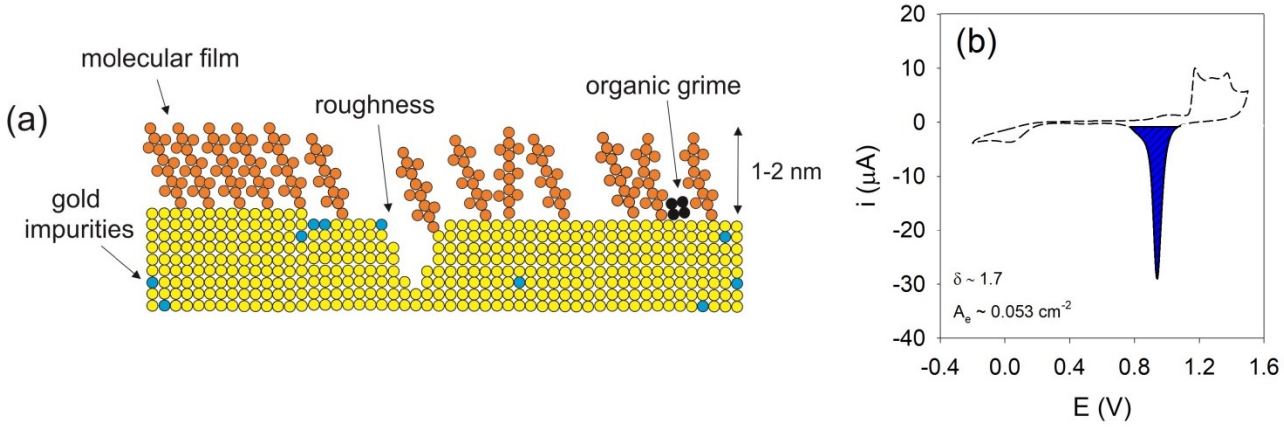

Figure 1. (a) Types of defects existing in a gold surface modified with a molecular layer. (b) Cyclic voltammetry measurements of a gold-disk electrode in 0.5 mmol L^{-1} H_2SO_4 aqueous solution (25th cycle). The electrochemical polishing was performed at a sweep rate of 0.1 V s^{-1} between -0.2 V to 1.5 V. Surface roughness factor was calculated by the mathematical integration of the peak hatched in blue (reduction of the gold oxide layer formed during the anodic scan). The obtained $\boldsymbol{\delta}$ was of 1.7 and the obtained electro-active area was calculated as 0.053 cm^{-2} from the geometric capacitive values of the interface.

Calculations of δ are based on the assumption that an atomic oxygen layer is chemisorbed over gold[36], which can be affected the fractal character of the surface as has been evidenced in references[47-49]. It follows the minimum electric current measured from the gold oxidation peak inferred from electrochemical measurements of electric current *versus* potential curves. This minimum electric current is usually taken as an indication (and theoretical referential value) that an oxygen monolayer coverage over gold surface is reached (deviations are discussed in references[23, 50]). The experimental value of the corresponding charge required for the reduction of this monolayer (see Figure 1, measurements conducted in sulphuric acid, blue hatched area) depends on the composition of the exposed crystalline planes. Values between 400 μC cm^{-2} to 482 μC cm^{-2} have been used as a referential range of value to estimate δ for polycrystalline gold surfaces[36]. Consecutive reduction of a gold surface is known as electro-polishing and sometimes is offered as a way of smoothing a metallic surface.

Though above-mentioned methodologies of estimating surface roughness are prone to flaws, particularly those that measure δ using electrochemical methods are quite useful. Providing that the cleaning procedure of the gold surface is efficient, these methods are quite effective for obtaining information of the surface at an atomic level. δ can be estimated by measuring the capacitance of the interface. The capacitance of a metal-electrolyte interface can be theoretically estimated using the Gouy-Chapman model[51] where an ionic capacitance (which is a generalization of the double-layer capacitance) per unit of geometric area is defined as $C_i = \varepsilon_r \varepsilon_0 \kappa$, where ε_0 and ε_r are the dielectric permittivity of vacuum (c.a. 8.85 x 10^{-12} F m^{-1}) and the relative static permittivity of the dielectric molecular or ionic layer[17, 52, 53] formed over a metallic surface, respectively. κ is the inverse of the Debye length ($\lambda_D{}^{-1}$). Debye length is defined as $\lambda_D = [(2e^2N)/\varepsilon_r \varepsilon_0 k_B T)]^{-1/2}$, where N is the density of ions (positive and negative in mol L^{-1}) in the bulk of the supporting electrolyte, k_B is the Boltzmann constant and T is the absolute temperature. The value of C_i (not normalized per unit of area) can be written as a function of δ as[14, 52, 53]

$$C_i = \varepsilon_0 \varepsilon_r \lambda_D^{-1} \delta. \quad (2)$$

Providing that electrolyte concentration does not change, then λ_D^{-1} is a constant and in this situation C_i is predicted to vary linearly with and proportionally to δ. Owing to the fact that C_i is experimentally measured, Eqn. (2) offers a useful way of obtaining δ for different types of surfaces. It is important to bear in mind that electro-polishing process uses electrochemical reduction of the interface so that it removes material and improves significantly a surface roughness at the atomic scale, but this process does not improve the texture of the surface, i.e. it does not affect the morphology of the surface. For instance, if a material surface has a texture or scratch, electro-polishing will only result in a lustrous texture or a lustrous scratch. Mechanical polishing must be utilized to remove macroscopic texture or blemishes.

The main goal of this work is to demonstrate the importance of controlling the roughness of a metallic surface as a quality control to fabricate molecular-based label-free biosensors or to perform fundamental studies of molecular assembling into solid surfaces. Particularly, it is noteworthy to control δ especially if researchers are aiming at to use steady-state techniques such as impedance or impedance-derived capacitance spectroscopies, where the imperfections of the interface are notable owing to the precision and spectroscopic characteristics of the method[54]. These techniques[54] are very sensitive and require a good quality control for the stability (and the reproducibility of the electrical response) of molecular assembles, which are essential for constructing and developing reliable interfaces within embedded electro-analytical transducer signals for diagnostic assays. The analysis made in this work demonstrates how essential is the control of the roughness of an interface to fabricate reliable printed circuit board (PCB) electrodes for label-free electrochemical biosensors.

Experimental procedures

Reactants and electrochemical measurements

All chemicals were purchased from Sigma-Aldrich, unless stated otherwise. The electrochemical potentials in this work are referred with respect to Ag|AgCl reference electrodes. Electrochemical measurements were conducted using a µAUTOLAB III / FRA 2 (Metrohm, The Netherlands) potentiostat and an AUTOLAB equipment with a Frequency Response Analyser (FRA) module; the latter is used for impedance measurements. All electrochemical data were obtained at room temperature (298 K). Basically, two types of electrodes were used: (a) gold-disk electrodes and (b) PCB micro-fabricated, gold electroplated electrodes where different strategies were used to control the roughness of the gold surface or to modify the surfaces with a molecular scale film.

Gold-disk electrodes

Firstly, the main requirement to be stated is the quality of the gold material. The gold to be used in the working electrodes must be as much pure as it can be. This is because, in ideal situations, the molecular attachment over gold electrodes would occurs at the ratio of one molecule per atom of gold existing in the surface (especially in the case of thiolated monolayers) and thus the purity of the gold is of a major importance to avoid unwanted defects. 10^{12} molecules per centimetre square mean a value of billions of times lower than a mole of molecules and few amounts of impurities can cause a great impact on the chemical properties of a molecular layer and thus changes can be huge as doping and impurities are for governing the properties of semi-conductors. For the required quality to be achieved we use 2 mm (in diameter) METROHM (assembled in PEEK) gold-disk electrodes which seems to work better comparatively to other electrodes tested by our groups – succeed in fabricating

requires a good sealing up of the gold into peek, for instance). METROHM gold-disk electrodes which have good quality regarding gold purity and sealing were initially polished mechanically using aluminium oxide with different particle sizes (1 µm, 0.3 µm, and 0.05 µm) aiming to obtain a range of A_e. Sonication in water was applied after polishing to remove adhered particles. Subsequently, the gold-disk electrodes were electrochemically polished in deaerated NaOH 0.5 M (from −0.7 to −1.7 V at a scan rate of 100 mV s^{-1}) and after that they were deaerated in 0.5 M H_2SO_4 (50 cycles from − 0.2 to + 1.5 V at a scan rate of 100 mV s^{-1}).

The integration of the cathodic peak obtained in gold electro-polishing voltammetric procedures, as obtained in sulphuric acid, was used to calculate A_e by means of applying a conversion factor of 410 µC cm^{-2}. After electro-polishing procedures the surface were characterized by electrochemical measurements including impedance spectroscopy. For electrochemical impedance measurements it was used frequencies ranging from 1 MHz to 100 mHz at bias potentials ranging from 0.2 V to 0.3 V with a step of 20 mV. The AC amplitude sinusoidal perturbation voltage was 20 mV (peak-to-peak). 12 mM phosphate buffered at pH 7.4 in 0.5 M KNO_3 was used as an electrolyte and the measurement at each potential was repeated three times. C_i was calculated from impedance analysis by converting complex impedance into capacitance using the following relationship $C^* = 1/j\omega Z^*$, where $j = \sqrt{-1}$ and $\omega = 2\pi f$ and these measurements were performed in the absence of a redox probe in solution. Finally, the real and imaginary components of the complex capacitance were obtained as $C' = 1/j\omega\, Z''$ and $C'' = 1/j\omega\, Z'$, respectively. This allows constructing Bode and Nyquist capacitive diagrams from where C_i [according to Eqn. (1)] was obtained.

To study the effect of the roughness factor of the gold interface over the electronic blocking properties of the surface, dodecanethiol monolayers were self-assembled over the surface of gold-disk electrodes and the redox performance (the ability the interface has to exchange electrons) was evaluated by electrochemical measurements in solution containing redox probe. The incubation time for monolayer to assembly was c.a. 12 h, and the electrochemical measurements (EIS and CV) were performed in $K_3Fe(CN)_6$ and $K_4Fe(CN)_6.4H_2O$, both at the concentration of 1 mM with a KNO_3 supporting electrolyte (1 M). The main circuit element evaluated during the studies of the electronic blocking effect was the charge transfer resistance (R_{ct}).

PCB electrodes

These types of electrodes were designed in PCB CAD software (Altium®) and fabricated in a standard PCB manufacturing facility. The copper layers were electroplated with a hard-gold finish in order to exploit the pore-free deposition and low contact resistance achieved by this technique. The METALOR® ENGOLDTM 2015CVR (Inc) process was followed, providing 2.41 µm gold on top of 3.41 µm Ni. Because certain PCB substrates are not allowed to be exposed to acid environments, cleaning and smoothing of surfaces was not possible to be made by using the electrochemical polishing methodology as was used in gold-disk electrodes. Alternatively, the PCB surfaces were treated with oxygen plasma (O_2, 80°C, 30 minutes) to remove organic contaminations and the surface roughness was evaluated using Eqn. (1), where the y_i th elements were assessed by AFM (Bruker Multimode IIIa) in tapping mode. AFM tips were obtained from BudgetSensors Tap150Al-G, soft tapping AFM tips with a resonant frequency of 150 kHz. The chemical purity of the Au electrode surfaces after the plasma treatment was characterized using X-ray Photoelectron Spectrometer, XPS. The spectra were recorded on a Thermo Scientific

K-Alpha-plus XPS system operating at $2x10^{-9}$ mbar base pressure. XPS data were analysed using the Avantage software package.

Additionally, the PCB electrodes were electrochemically characterized as working electrodes (each of them containing a geometric area of ca. 0.02 cm^2) in an electrolyte environment. Cyclic voltammograms (CVs) were recorded to compare the electrochemical performance of PCB electrodes possessing different surface roughness. The CVs were acquired in PBS solution containing 4 mM $K_3Fe(CN)_6$ in 50 µL of PBS sample.

PCB electrodes modified with a composite

Note that a redox-composite can serve as a chemical modifier of a micro-fabricated PCB electrode. If they possess suitable thickness characteristics that can assure an easier translation of physical properties developed in a gold-disk electrode to the surface of a micro-fabricated PCB electrode. Indeed, because of the larger thickness of composite compared to the traditional monolayers, the composite is able to accommodate any remaining roughness issues associated with the PCB electrode[55]. The chemical modification of the electrode with the composite consisted of the following steps: first, a self-assembled monolayer was generated by immersing freshly cleaned gold-disk in an ethanol (HPLC grade) solution of 2.0 mM of 11-ferrocenyl-undecanethiol (11-FcC) for 16 h. Subsequently, the surface 11-FcC modified electrodes were rinsed with absolute ethanol and dried in a flow of nitrogen gas before incubation in an aqueous solution of 2 mg mL^{-1} graphene oxide (GO) overnight at room temperature in a glove box. The modified gold-disks were placed into a reaction tube sealed with rubber septum stoppers before removal from the glove box. Then, 25 mL of a degassed solution of 7.5 mmol of CBMA zwitterionic monomer [2-carboxyN, Ndimethyl-N-(2'-methacryloyloxyethyl) ethanaminium inner salt] dissolved in H_2O/methanol solvent (1:1 volume ratio) was transferred to the tube using a syringe and kept under agitation (using a magnetic stirrer) with nitrogen protection by 8 h. After the formation of the redox-composite, the modified gold-disks were removed and rinsed with H_2O/methanol, H_2O and then dried with N_2 flow. The carboxylate groups (presents in both GO and CBMA) were activated by 1-Ethyl-3-(3-dimethylaminopropyl) carbodiimide (EDC)(0.4 M) and N-Hydroxysuccinimide (NHS) (0.1 M) for 40 min, followed by incubation in 1 µM CRP antibody PBS solution overnight at 4 °C. The thickness of the redox-composite was determined by ellipsometry.

Results and discussion

Roughness factor and electrochemical characterization of gold-disk electrodes

Gold-disk electrodes were mechanically and coarsely polished using 1 µm particle-sized; moderately polished by using decreasing 1 µm and 0.3 µm particle-sized; and subsequently, finely polished applying 1 µm, 0.3 µm, and 0.05 µm. C_i, which was independently calculated by using EIS measurements, where plotted as a function of δ values. Calculation of δ values were described in the experimental procedure (see also Figure 1) and varied from 1.4 to 2.7. Figure 2 shows Nyquist capacitive diagrams from where C_i were obtained as the value of the diameter of the semi-circle (Figure 2*a*) and plotted as a function of different δ values obtained by different quality of electrochemically polished METROHM gold-disk electrodes. Note that, as discussed in the SI document, fitting procedures using equivalent circuits bring the same trends as using a simple graphical analysis. The behaviour observed in Figure 2 is predicted and in agreement to Eqn. (2).

Figure 3*a* shows C_i as a function of δ ($C_i \propto \delta$) across different potential, i.e. between 0.2 V to 0.3 V. From this figure, it can be inferred that $C_i \propto \delta$ decreases almost linearly from lower to higher positive potentials. This linear behaviour is independent of the degree of δ, suggesting that there is a correlation of the electric potential at the interface with the ionic concentration therein. The linear relationship of C_i obtained as a function of δ and predicted by Eqn. (1) was confirmed only for capacitive values obtained in potentials between 0.28 V to 0.30 V. Also, the linearity between C_i and δ remains only for δ values stated between 1.4 and 1.8. For δ values greater than 1.8 we suggest that the arbitrary behaviour is likely due to the formation of multiple oxide layers over the surface of the gold and, therefore, the criteria to obtain δ by using a conversion factor of 410 µC cm^{-2} (or other equivalent value as a reference) is no longer obeyed. The predicted linear relationship between C_i and δ is no longer obtained if any oxygen/Au stoichiometry is not predictably controllable to the charge.

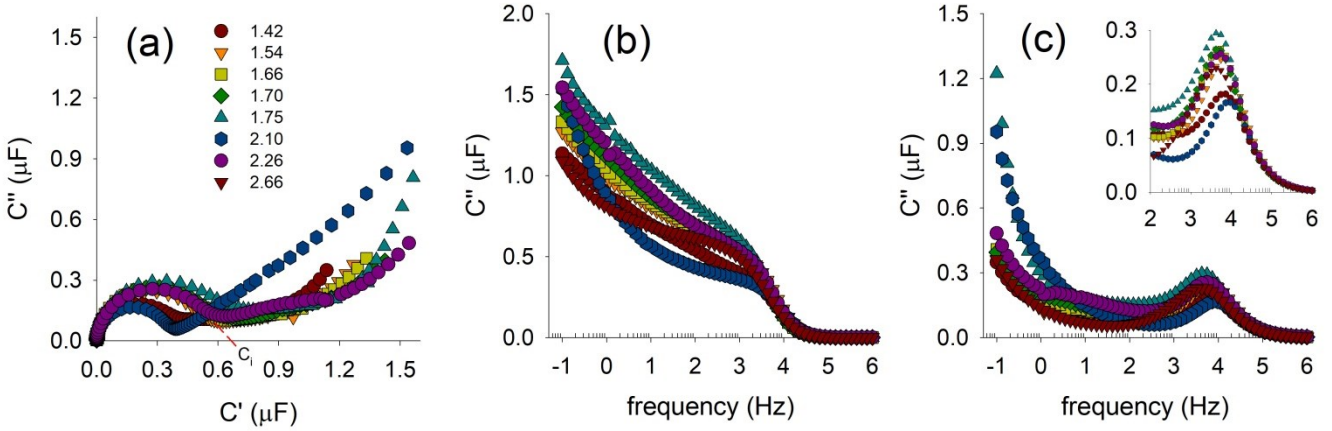

Figure 2. (a) Nyquist plots showing the capacitive fingerprint of gold-disk electrodes due to different roughness factors (see legend). (b) and (c) are the bode plot showing the real ($\boldsymbol{C}$') and imaginary ($\boldsymbol{C}$") capacitance (presented in "a") against the linear frequency range. $\boldsymbol{C_i}$ is obtained as the diameter of the semicircle as indicated in (a). EIS measurements were performed at 0.28 V using 12 mM PB at a pH of 7.4 in 0.5 M of KNO_3.

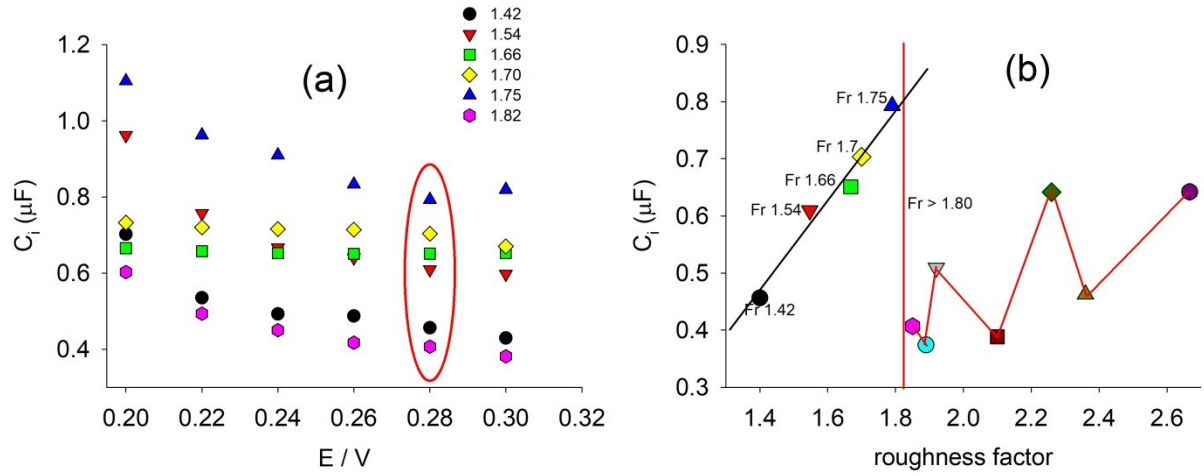

Figure 3. (a) The effect of roughness factor observed in ionic capacitance across a range of potential between 0.2 V to 0.3 V. (b) At the 0.28 V a predicted linear relationship [see Eqn. (2)] is obtained between $\boldsymbol{C_i}$ and $\boldsymbol{\delta}$ for values of roughness factor lower than 1.8. Note that a randomized pattern is observed for values of roughness factor higher than 1.8 for which the linear relationship between $\boldsymbol{C_i}$ and $\boldsymbol{\delta}$ can no longer be attained. Note, in the SI document, that the use of the graphical analysis, to obtain the capacitance, is quite reliable when

compared with the fitting procedure. The trend observed in this figure is independent of the mathematical method used to extract the capacitance values of these interfaces.

Surface roughness effect on electrochemical reversibility of PCB electrodes

In this section, we evaluate the impact of surface roughness on the electrochemical or the redox reversibility of gold-plated PCB electrodes. The surface roughness was determined following Eqn. (1) after the plasma cleaning procedure. Note that the method used in Eqn. (1) is different from that of Eqn. (2) and a theoretical correlation between them has not been established yet. The redox reversibility of PCB electrodes after plasma cleaning were attained by measuring peak potential differences (ΔE) between reduction and oxidation processes of a $K_3Fe(CN)_6$ redox probe (Figure 4). The electrochemical reversibility was compared with the surface roughness that was obtained by AFM measurement (Figure 5) and by applying Eqn. (1). Figure 4*a* shows a reasonably reversible electrochemical activity as inferred from cyclic voltammogram pattern of $K_3Fe(CN)_6$ redox probe when the electrode's surface roughness falls in between 18 nm and 40 nm. It is clearly observed that the electrochemical reversibility of PCB electrodes behaves differently depending on the roughness of the surface. Surface roughness between 18 nm and 40 nm has a suitable redox reversibility which demonstrates that these substrates can be used for the assembling of molecular scale films. On the other hand, electrochemical irreversibility increases (Figure 4*b*) for gold-micro-fabricated PCB electrodes containing surface roughness higher than 40 nm. The electrochemical irreversibility encompasses electrodes that are only moderately suitable for the assembling of molecular layers over them. The irreversibility also depends on the molecular film thickness as will be demonstrated further herein, because the higher the molecular film thickness, the lower the impact of roughness on the electrochemical response. In other words, the use of electrochemical reversibility as a quality factor of surface roughness allows us to take values of roughness factor as a parameter of quality.

In summary, this criterion allows us to classify the quality of surfaces for the assembly of molecular films over them. Roughness lower than 40 nm are suitable. Nonetheless, when they are in between 41 nm to 50 nm they are not recommended and surface roughness higher than 55 nm generates poor quality surface for molecular assembly. Interestingly, we observed that the gold-micro-fabricated PCB electrodes encompassing surface roughness higher than 70 nm are not redox active and so the electrochemical irreversibility is quite poor (not shown).

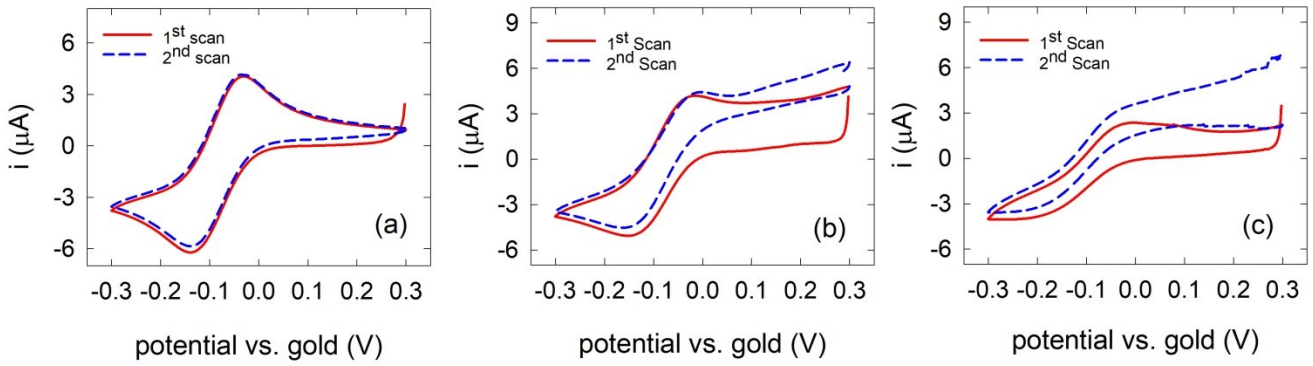

Figure 4. Cyclic voltammograms of PBS solution containing 4 mM $K_3Fe(CN)_6$ at commercially fabricated PCB to be used as sensing platform. (a) good, (b) intermediate, and (c) poor electrochemical reversibility.

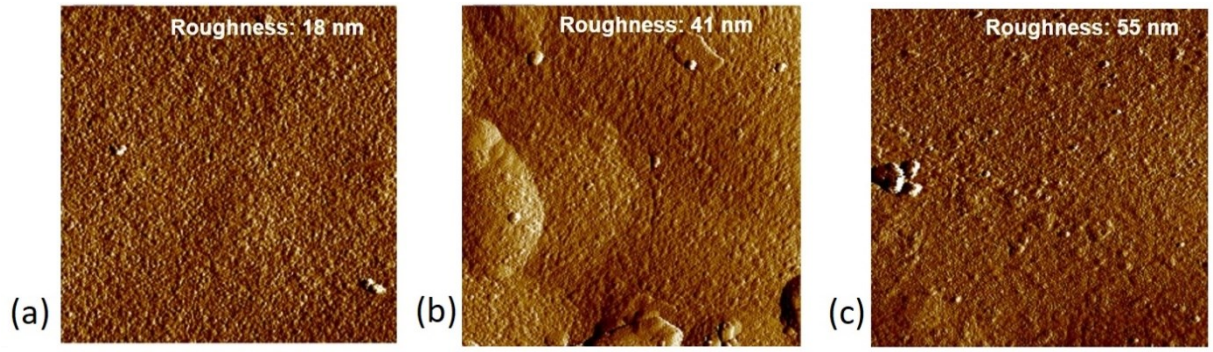

Figure 5. Atomic force micrographs of (a) good, (b) intermediate, and (c) poor electrochemical reactivity of plasma cleaned PCB that is aimed at sensing applications. The scan size is of 2 µm × 2 µm.

The redox reversibility of gold-micro-fabricated PCB electrodes can be quantified by ΔE values, allowing a more systematic study of the impact of surface roughness in the electrochemical activity. Indeed, a very clear logarithmic relationship between ΔE and surface roughness was observed (Figure 6*a*). ΔE values increased exponentially-like as a function of the increase of surface roughness. This is clearly an indication that rougher surfaces correspond to lower redox reversibility.

The chemical purity effect of the electrode surfaces was also performed in order to identify whether it is the mechanical surface roughness of the electrodes that controls the redox reversibility characteristics of the surface or whether there is a synergistic effect with the chemical composition. Hence, the XPS spectra of Au, Cu, C, O, N and F of the PCB electrodes' surfaces were measured after the plasma cleaning procedure. Figure 6*b* shows a comparative plot of the Au:Cu:C:O:N:F ratios derived from XPS measurements versus ΔE. No relationship between surface element composition or contamination and redox reversibility was found. This reinforces our previous observations that the origin of the redox activity is undeniably associated mostly with the geometric roughness of the surface.

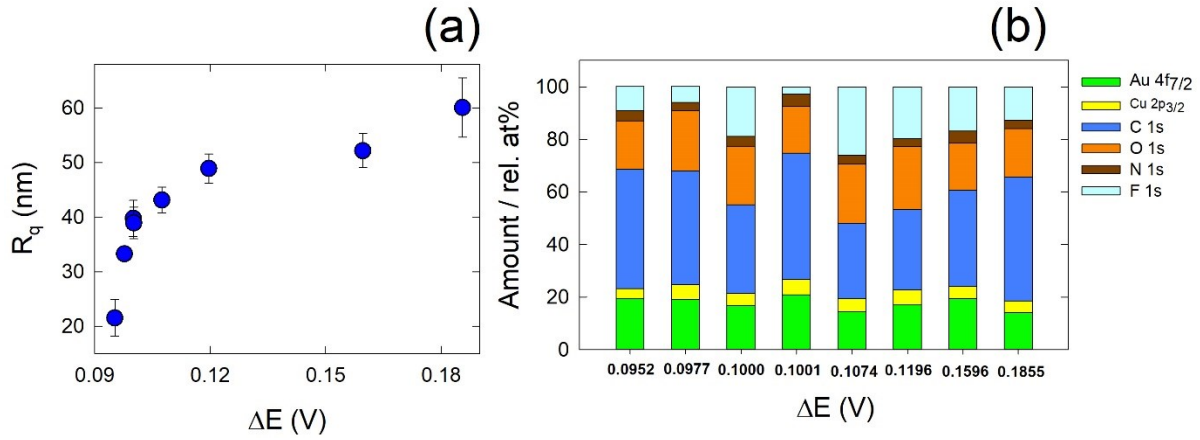

Figure 6. (a) ΔE obtained from cyclic voltammograms and its dependence on the roughness of PCB sensing electrodes. (b) Comparative plots of the Au:Cu:C:O:N:F ratios derived from XPS measurements on the surface of the printed circuit board sensing electrodes on the ΔE of cyclic voltammograms.

Surface roughness and dielectric blocking effect

The effects of the roughness factor on the blocking of redox activity of a molecular film will be evaluated in this section and correlated to the results of capacitance of the interface as obtained without the formation of molecular films over it. It is well-known that dielectric monolayers self-assembled over metallic interfaces cause an electronic blocking effect for the transfer of electrons from the solution to the electrode and vice-versa[52]. The quality of the arrangement of the molecular interface and defects on it, as illustrated in Figure 1, impacts on the redox reaction activity, causing a suppress and a decrease of redox reaction rate. This can be qualitatively evaluated by CV measurements as shown in Figure 7, where it is demonstrated, comparatively, the responses of a bare gold surface and the same surface after the assembling of a molecular dielectric layer containing 12 carbons over it (an estimated thickness of c.a. 1.2 nm). As can be seen in this figure, the lower the roughness [from (a) to (d)] the higher the blocking effect of the interface on the redox activity, which is qualitatively observed as a suppression of the redox peak current and of the redox activity of the interface as a whole. In other words, the roughness of the surface decreases the quality of the monolayer arrangement and of the molecular packing and so it impacts on the blocking ability of the molecular film to transfer electrons to/from the electrode from/to the redox species in solution. A poor molecular arrangement reflects in a higher probability of electron transfer to occur through alternative (percolation) paths in the monolayer and so the electrochemical current is higher, in the presence of a redox probe in solution, for those interfaces where blocking dielectric molecular monolayers were assembled over rough surfaces.

Table 1. Values of charge transfer resistance obtained for different molecular films assembled into different roughness surfaces. Higher roughness leads to a non-reproducibility or to a random electrochemical response as a function of the roughness. In agreement with capacitance behaviour of the interface, which is a function of the roughness, roughness factors lower than 1.8 leads to a more consistent and repeatable electrochemical responses of the junctions. These are values obtained from triplicates.

$\delta > 1.8$	R_{ct} (kΩ cm^2)	$\delta < 1.8$	R_{ct} (kΩ cm^2)
1.9 ± 0.3	6.3 ± 1.2	1.2 ± 0.2	3,441 ± 187
2.9 ± 0.2	178.1 ± 30.3	1.4 ± 0.2	3,637 ± 142
11.1 ± 0.3	15.5 ± 6.1	1.1 ± 0.1	3,413 ± 168

A better evaluation (than qualitative CV measurements) is made by using EIS quantitative measurements as shown in Figure 8. This particular experimental situation can be modelled by using a Randles-like equivalent circuit[52, 53, 56, 57], allowing us to extract useful quantitative parameters to be studied. For instance, equivalent circuit analysis of the interface is made by fitting the results with a Randles-like circuit[56, 57] and from this analysis, the most important parameter to be obtained and where we will be focused in the following discussion is the charge transfer resistance, i.e., R_{ct}. The EIS results, as shown in Figure 8, are in agreement and reinforce the CV analysis. Accordingly, it can be noted that for $\delta \sim 1$, the R_{ct} is higher than for those values of roughness factor above 2. For instance, it can be observed that for a $\delta \sim 2.6$, a R_{ct} of 5.0 kΩ cm² is obtained (Figure 8*a*), meanwhile for the case where $\delta \sim 1.05$ the obtained R_{ct} is three orders of magnitude higher, i.e., $>$ 3,000 kΩ cm^2 (Figure

8*d*). Undoubtedly, these results are showing that δ has a significantly impact on the electrochemical responses of molecular films formed on gold surfaces.

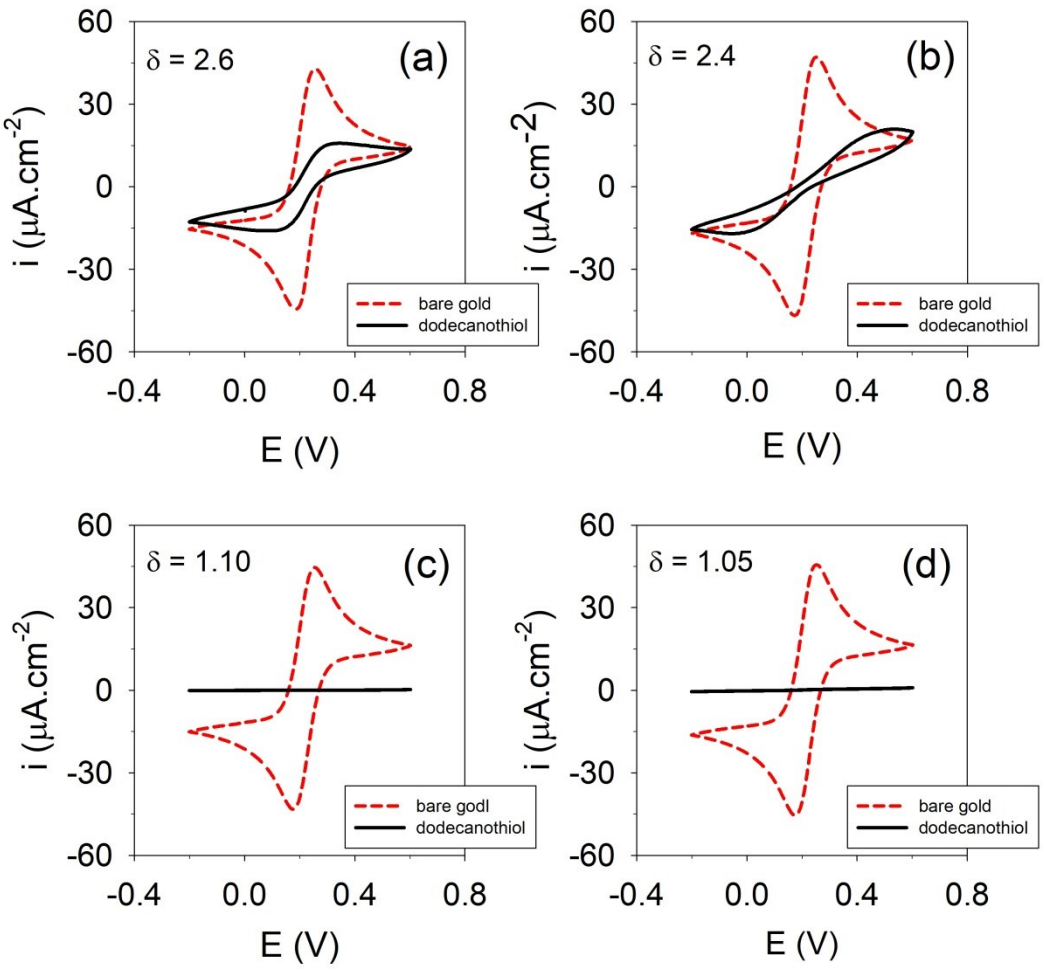

Figure 7. Cyclic voltammograms reflecting the quality of a dodecanethiol molecular film formed over bare gold as a function of roughness factor of that interface. Roughness factor increases from (a) to (d).

Indeed, this simple equivalent circuit analysis is reflecting the geometric characteristics of the gold interfaces which were preliminarily evaluated using a capacitive analysis of the interface. In the capacitive analysis (Figures 2 and 3) we demonstrated that for $\delta > 1.8$, the capacitive response of the interface is unsystematic. Equivalently, this unsystematic characteristic of the response can be observed quantitatively in Table 1, where for $\delta > 1.8$, the R_{ct} is random. On the other hand, for $\delta < 1.8$, the R_{ct} is consistently about 3,500 kΩ cm^2, which confirms that a certain and minimum control of the roughness factor is needed to design consistent and reproducible molecular scale junctions. In the next section we will show how we can use this information to translate the properties of a gold-disk interface used to made molecular assays into a potentially commercial useful platform than are the gold-disk electrodes.

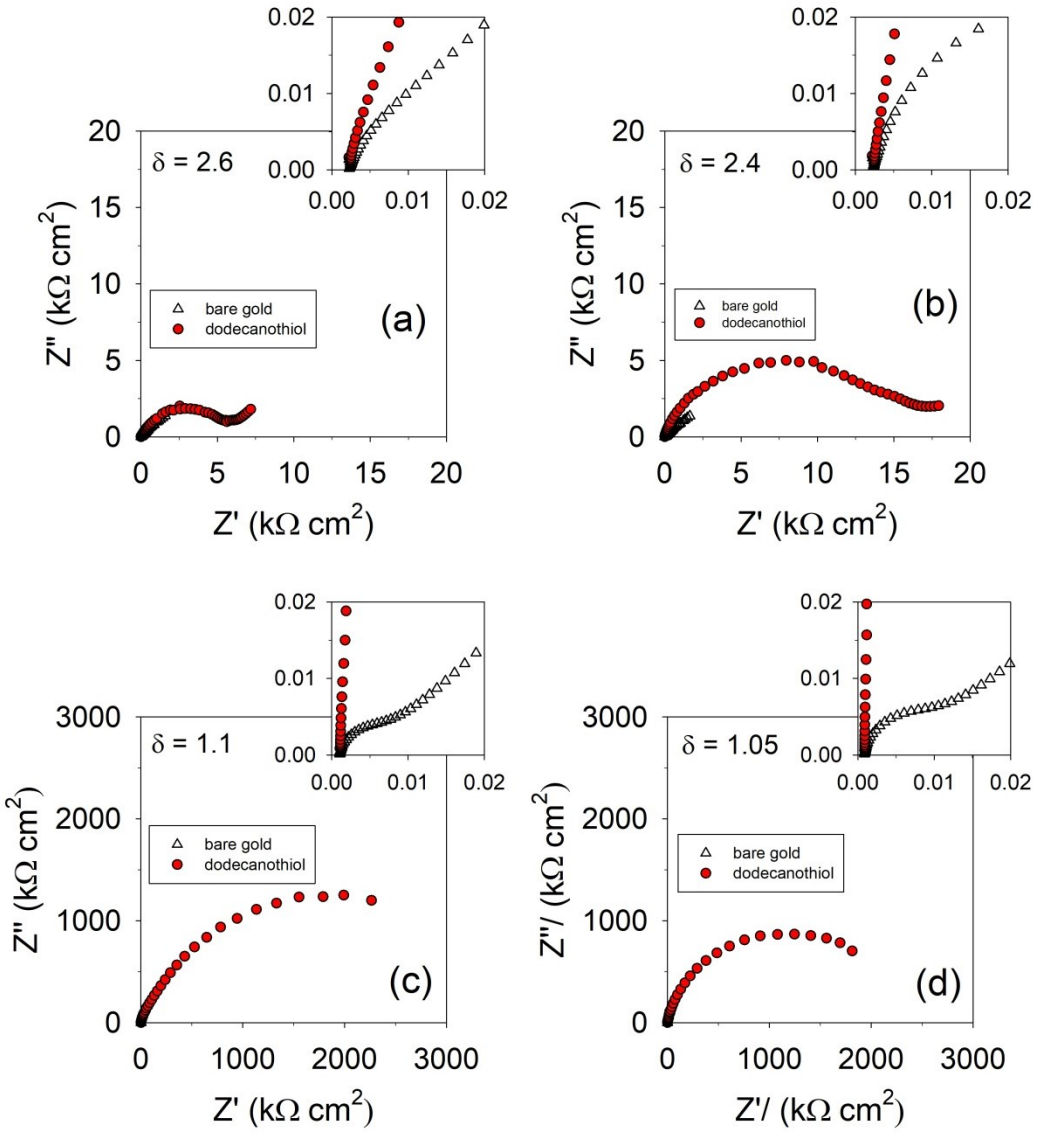

Figure 8. Impedance measurement in the presence of the redox probe in a solution made in a dodecanethiol molecular film formed over bare gold as a function of roughness factor of that interface. Roughness factor increases from (a) to (d).

Comparisons between the gold-disk and PCB electrode performance in biosensor applications

At this stage, it will be demonstrated that the performance of a gold-disk electrode can be reproduced in a PCB electrode platform whether the roughness of the surface is controlled in levels lower than 20 nm as estimated from Eqn. (1). This is required to obtain stable film (and a time-invariant interface that allows impedance to be appropriated used), avoiding drift that can lead to false positive results[54]. For instance, Figures 9*a* and 9*b* specifically show how the resolved responsiveness of a redox capacitive signal at the interface containing anti-CRP antibody can be converted from a gold-disk electrode to a gold micro-fabricated PCB electrode platform. The redox capacitive signal is different of the ionic capacitance. Ionic capacitance, as previously introduced in the present work, is a non-Faradaic capacitance while the redox capacitance encompasses Faradaic (pseudo-

capacitive) contributions. More details of redox capacitance and its using in biosensing devices can be found in references[14, 15].

If the chemistry of a redox capacitive molecular film is made of a composite (Au/11-FcC/GO/CBMA), details can be found elsewhere[18, 55], instead of the monolayer (more details also are given in the experimental section), with higher thickness, such as c.a. 9-10 nm thickness (as measured by ellipsometry – not shown). This surface has been shown to be suitable for assaying clinically relevant levels of CRP both at gold-disk and PCB electrodes[18, 55] by using the redox capacitance signal of the interface. The redox properties of the interface are assured by adding 11-ferrocenyl-undecanethiol (11-FcC) to as part of a composite which slightly allows thickness to increase from c.a. 1.2 nm (if a monolayer of 11-FcC) to c.a. 9-10 nm (when the composite is used in the interface). This redox composite within larger thickness compared to a self-assembled monolayer is able to retain the mesoscopic characteristic needed for the interface. By mesoscopic characteristics here we mean an interface that has one of its dimensions at a nanoscale lower than 10 nm (the thickness at this case), allowing it to retain certain degree of quantized characteristics that allow some pseudo-capacitive (which is here referred as redox capacitance) effects to prevail over the geometric capacitance of the interface. The latter is, for instance, a useful situation that allows to improve the capacitive sensitiveness of the interface and to use of the amplified capacitive signal[58, 59] as transducer to biological events occurring at the interface.

Finally, this CRP recruiting interface (Au/11-FcC/GO/CBMA/Ab-CRP) were immersed in 1 M ethanolamine (pH of 8.5) for 5 minutes to deactivate any unreacted activated carboxylic groups and washed with PBS prior to measurements. Each step of the fabrication of receptor interface was characterized by cyclic voltammetry and impedance-derived capacitance analysis (the measurements were conducted in a supporting electrolyte of 20 mM $TBAClO_4$ following the procedures indicated elsewhere[18]). The formal potential of this interface was found as to be 0.45 V. This receptive surface was tested against CRP at concentrations ranging from 50 pM to 5 x 10^4 pM in PBS (R-squared of 0.980) (Figure 7*a*). The sensitivity was 8.6 % conc.$^{-1}$ with LoD of 21.6 ± 5.2 pM (with the errors corresponding to an average of three assays made at the same electrode).

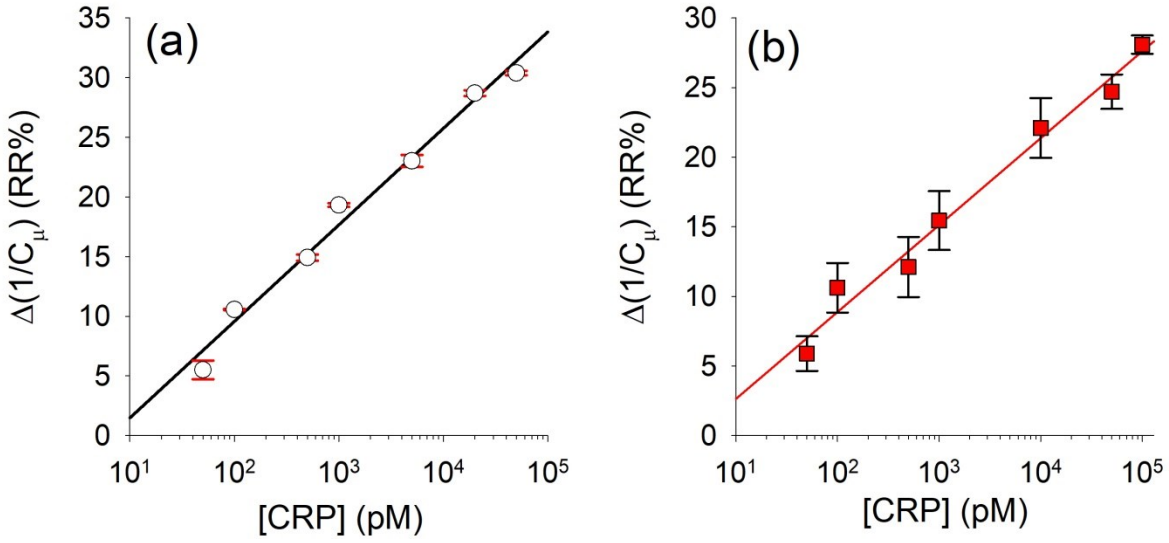

Figure 9. The relative linear (%) response of $1/C_\mu$ at the formal potential of a molecular film containing CRP receptive moieties and redox active groups. The relative response is linear with the logarithm of concentration of CRP, as expected theoretically[14, 15]. (a) gold-disk

electrodes (METROHM) wherein errors bar the are standard deviations associated to three measurements at the same electrode (LoD of 21.6 ± 5.2) and (b) gold-micro-fabricated PCB electrodes with errors bar as the standard deviations across three different electrodes (LoD of 16.8 ± 1.2 pM). These results confirmed that surfaces prepared at gold-disk electrodes can be translated into micro-fabricated disposable electrodes aiming at sensing applications. Note in the SI document (section S3) that if the roughness factor is not controlled, the best as possible analytical curve constructed by selecting the three best electrodes among 10 to 15 presents a much higher deviation and error bar.

This optimized redox-composite (used in Figure 9*a*) was applied to gold micro-fabricated PCB electrodes and were rinsed with ethanol and washed with water prior to electrochemical pre-treatment in 0.5 M H_2SO_4 using cyclic voltammetry (−0.2 to 1.6 V at a scan rate of 1 V s – up to 100 cycles) until a stable sharp peak (FWHM ∼90 mV) is obtained. To assure the proper translation of the receptive interface from gold-disk (measurements shown in Figure 9*a*) to gold-micro-fabricated PCB electrodes the latter was tested in PBS environment following previous procedures (measurements are shown in Figure 9*b*) applied to modified gold-disk electrodes containing redox-active groups. The obtained LoD was of 16.8 ± 1.2 pM across three different electrodes which are quite similar to the LoD of 21.6 ± 5.2 obtained in gold-disk electrodes. The LoD obtained in serum was resolved as 56.4 ± 7.8 pM. To attest the specificity this receptive interface was incubated with human serum albumin (HSA from Sigma-Aldrich) in PBS with HSA at concentrations ranging from 50 pM to 100 nM wherein the relative response in percentage $1/C_{\bar{\mu}}$ oscillated between -2.2 ± 1.0 % to 1.6 ± 1.7 % (inside of the noise of equipment and are within experimental error of the measurements).

In summary, the use of a nanostructured composite (of about 10 nm, which still prevent the presence of diffusive effects to the transport of charge) as a redox capacitive interface for detection of CRP was successfully implemented in gold-disk electrode and PCB electrodes. The implementation of a label-free capacitive platform using field-based PCB electrodes is of great interest for point-of-care applications.

Conclusions

In this work we demonstrated that surface roughness as obtained by both mechanical and electrochemical methods can be used as quality control for the reliable assembly of molecules over electrodes with the purpose of chemically engineering surfaces aiming at to molecular diagnostic applications. Most important, the control of the roughness factor of the surface allows us to improve reproducibility and stability of the sensing interfaces. It was demonstrated that the control of the roughness factor permits us to translate assays developed in academic laboratories into commercially viable PCB electrodes aiming at label-free capacitive point-of-care assays. The translation of laboratory platform to PCB electrodes was here practically demonstrated by using CRP assays. The CPR assays were attained using serum samples. CRP assays performed in the surface of PCB-based electrodes shown suitable electroanalytical parameters that can compete to those performed over gold-disk electrodes. The latter is particularly the case where effects associated with the surface roughness of the PCB substrate are compensated or overcome by the higher thickness of a modified composite film assembled over it.

Acknowledgments

The authors acknowledge Dr. Anna Regoutz to provide XPS raw data. Also, the authors gratefully acknowledge the financial support of FAPESP (PRINT and 2017/24839-0 thematic project) and of the University of Bath International Funding Scheme and the British Council (Newton Fund Institutional Links, UK-Turkey project

336872). PRB would also like to kindly recognize the graduate students of the group in providing raw data that illustrate some parts of this manuscript.

References

1. Chan, M.; Esteve, D.; Escriba, C.; Campo, E., A review of smart homes - Present state and future challenges. *Computer Methods and Programs in Biomedicine* **2008,** *91* (1), 55-81.
2. El-Ali, J.; Sorger, P. K.; Jensen, K. F., Cells on chips. *Nature* **2006,** *442* (7101), 403-411.
3. Halik, M.; Klauk, H.; Zschieschang, U.; Schmid, G.; Dehm, C.; Schutz, M.; Maisch, S.; Effenberger, F.; Brunnbauer, M.; Stellacci, F., Low-voltage organic transistors with an amorphous molecular gate dielectric. *Nature* **2004,** *431* (7011), 963-966.
4. Li, D.; Song, S. P.; Fan, C. H., Target-Responsive Structural Switching for Nucleic Acid-Based Sensors. *Accounts of Chemical Research* **2010,** *43* (5), 631-641.
5. Wang, J., Electrochemical biosensors: Towards point-of-care cancer diagnostics. *Biosensors & Bioelectronics* **2006,** *21* (10), 1887-1892.
6. Bogani, L.; Wernsdorfer, W., Molecular spintronics using single-molecule magnets. *Nature Materials* **2008,** *7* (3), 179-186.
7. Braun, E.; Eichen, Y.; Sivan, U.; Ben-Yoseph, G., DNA-templated assembly and electrode attachment of a conducting silver wire. *Nature* **1998,** *391* (6669), 775-778.
8. Bueno, P. R.; Davis, J. J., Charge transport and energy storage at the molecular scale: from nanoelectronics to electrochemical sensing. *Chemical Society Reviews* **2020,** *49* (21), 7505-7515.
9. Batzill, M.; Diebold, U., The surface and materials science of tin oxide. *Progress in Surface Science* **2005,** *79* (2-4), 47-154.
10. Holtz, J. H.; Asher, S. A., Polymerized colloidal crystal hydrogel films as intelligent chemical sensing materials. *Nature* **1997,** *389* (6653), 829-832.
11. Peppas, N. A.; Hilt, J. Z.; Khademhosseini, A.; Langer, R., Hydrogels in biology and medicine: From molecular principles to bionanotechnology. *Advanced Materials* **2006,** *18* (11), 1345-1360.
12. Robinson, J. T.; Perkins, F. K.; Snow, E. S.; Wei, Z. Q.; Sheehan, P. E., Reduced Graphene Oxide Molecular Sensors. *Nano Letters* **2008,** *8* (10), 3137-3140.
13. Shekhah, O.; Liu, J.; Fischer, R. A.; Woll, C., MOF thin films: existing and future applications. *Chemical Society Reviews* **2011,** *40* (2), 1081-1106.
14. Bueno, P. R., Common Principles of Molecular Electronics and Nanoscale Electrochemistry. *Analytical Chemistry* **2018,** *90* (12), 7095-7106.
15. Bueno, P. R., *The Nanoscale Electrochemistry of Molecular Contacts*. Springer: 2018.
16. Eckermann, A. L.; Feld, D. J.; Shaw, J. A.; Meade, T. J., Electrochemistry of redox-active self-assembled monolayers. *Coord. Chem. Rev.* **2010,** *254* (15–16), 1769-1802.
17. Bueno, P. R.; Benites, T. A.; Davis, J. J., The Mesoscopic Electrochemistry of Molecular Junctions. *Scientific Reports* **2016,** *6*.
18. Bueno, P. R.; Fernandes, F. C. B.; Davis, J. J., Quantum capacitance as a reagentless molecular sensing element. *Nanoscale* **2017,** *9* (40), 15362-15370.
19. Garrote, B. L.; Santos, A.; Bueno, P. R., Perspectives on and Precautions for the Uses of Electric Spectroscopic Methods in Label-free Biosensing Applications. *ACS Sens.* **2019,** *4*.
20. Boal, A. K.; Ilhan, F.; DeRouchey, J. E.; Thurn-Albrecht, T.; Russell, T. P.; Rotello, V. M., Self-assembly of nanoparticles into structured spherical and network aggregates. *Nature* **2000,** *404* (6779), 746-748.
21. Schreiber, F., Structure and growth of self-assembling monolayers. *Progress in Surface Science* **2000,** *65* (5-8), 151-256.

22. Smith, R. K.; Lewis, P. A.; Weiss, P. S., Patterning self-assembled monolayers. *Progress in Surface Science* **2004,** *75* (1-2), 1-68.
23. Vericat, C.; Vela, M. E.; Benitez, G.; Carro, P.; Salvarezza, R. C., Self-assembled monolayers of thiols and dithiols on gold: new challenges for a well-known system. *Chemical Society Reviews* **2010,** *39* (5), 1805-1834.
24. Fan, X. D.; White, I. M.; Shopova, S. I.; Zhu, H. Y.; Suter, J. D.; Sun, Y. Z., Sensitive optical biosensors for unlabeled targets: A review. *Analytica Chimica Acta* **2008,** *620* (1-2), 8-26.
25. Homola, J., Present and future of surface plasmon resonance biosensors. *Analytical and Bioanalytical Chemistry* **2003,** *377* (3), 528-539.
26. Sassolas, A.; Leca-Bouvier, B. D.; Blum, L. J., DNA biosensors and microarrays. *Chemical Reviews* **2008,** *108* (1), 109-139.
27. Wang, J., Nanomaterial-based electrochemical biosensors. *Analyst* **2005,** *130* (4), 421-426.
28. Willner, I.; Zayats, M., Electronic aptamer-based sensors. *Angewandte Chemie-International Edition* **2007,** *46* (34), 6408-6418.
29. Zhou, M.; Zhai, Y. M.; Dong, S. J., Electrochemical Sensing and Biosensing Platform Based on Chemically Reduced Graphene Oxide. *Analytical Chemistry* **2009,** *81* (14), 5603-5613.
30. Creager, S. E.; Hockett, L. A.; Rowe, G. K., Consequences of microscopic surface-roughness for molecular self-assembly. *Langmuir* **1992,** *8* (3), 854-861.
31. Hoogvliet, J. C.; Dijksma, M.; Kamp, B.; van Bennekom, W. P., Electrochemical pretreatment of polycrystalline gold electrodes to produce a reproducible surface roughness for self assembly: A study in phosphate buffer pH 7.4. *Analytical Chemistry* **2000,** *72* (9), 2016-2021.
32. Kolb, D. M., An atomistic view of electrochemistry. *Surface Science* **2002,** *500* (1-3), 722-740.
33. Schlenoff, J. B.; Li, M.; Ly, H., Stability and self-exchange in alkanethiol monolayers. *Journal of the American Chemical Society* **1995,** *117* (50), 12528-12536.
34. Walczak, M. M.; Alves, C. A.; Lamp, B. D.; Porter, M. D., Electrochemical and x-ray photoelectron spectroscopic evidence for differences in the binding-sites of alkanethiolate monolayers chemisorbed at gold. *Journal of Electroanalytical Chemistry* **1995,** *396* (1-2), 103-114.
35. Morozan, A.; Jaouen, F., Metal organic frameworks for electrochemical applications. *Energy & Environmental Science* **2012,** *5* (11), 9269-9290.
36. Trasatti, S.; Petrii, O. A., Real surface-area measurements in electrochemistry. *Pure and Applied Chemistry* **1991,** *63* (5), 711-734.
37. Millo, D.; Ranieri, A.; Gross, P.; Ly, H. K.; Borsari, M.; Hildebrandt, P.; Wuite, G. J. L.; Gooijer, C.; van der Zwan, G., Electrochemical Response of Cytochrome c Immobilized on Smooth and Roughened Silver and Gold Surfaces Chemically Modified with 11-Mercaptounodecanoic Acid. *Journal of Physical Chemistry C* **2009,** *113* (7), 2861-2866.
38. Bizzotto, D.; Burgess, I. J.; Doneux, T.; Sagara, T.; Yu, H.-Z., Beyond Simple Cartoons: Challenges in Characterizing Electrochemical Biosensor Interfaces. *ACS Sensors* **2018,** *3* (1), 5-12.
39. Dubois, L. H.; Nuzzo, R. G., Synthesis, structure, and properties of model organic-surfaces. *Annual Review of Physical Chemistry* **1992,** *43*, 437-463.
40. Finklea, H. O., Electrochemistry of organized monolayers of thiols and related molecules on electrodes. *Electroanalytical Chemistry: A Series of Advances, Vol 19* **1996,** *19*, 109-335.
41. Jolly, P.; Rainbow, J.; Regoutz, A.; Estrela, P.; Moschou, D., A PNA-based Lab-on-PCB diagnostic platform for rapid and high sensitivity DNA quantification. *Biosensors & Bioelectronics* **2019,** *123*, 244-250.
42. Moschou, D.; Tserepi, A., The lab-on-PCB approach: tackling the μTAS commercial upscaling bottleneck. *Lab on a Chip* **2017,** *17* (8), 1388-1405.
43. Cecchetto, J.; Santos, A.; Mondini, A.; Cilli, E. M.; Bueno, P. R., Serological point-of-care and label-free capacitive diagnosis of dengue virus infection. *Biosensors & Bioelectronics* **2020,** *151*, 111972.

44. 4287, B. E. I., Geometrical product specification (GPS). Surface texture. Profile method. Terms, definitions and surface texture parameters. 2000.
45. Coffinier, Y.; Piret, G.; Das, M. R.; Boukherroub, R., Effect of surface roughness and chemical composition on the wetting properties of silicon-based substrates. *Comptes Rendus Chimie* **2013,** *16* (1), 65-72.
46. Trasatti, S.; Petrii, O. A., Real surface-area measurements in electrochemistry. *Journal of Electroanalytical Chemistry* **1992,** *327* (1-2), 353-376.
47. Pajkossy, T., Electrochemistry at fractal surfaces. *Journal of Electroanalytical Chemistry* **1991,** *300* (1-2), 1-11.
48. Pajkossy, T., Impedance of rough capacitive electrodes. *Journal of Electroanalytical Chemistry* **1994,** *364* (1-2), 111-125.
49. Pajkossy, T., Impedance spectroscopy at interfaces of metals and aqueous solutions - Surface roughness, CPE and related issues. *Solid State Ionics* **2005,** *176* (25-28), 1997-2003.
50. Yan, L.; Huck, W. T. S.; Whitesides, G. M., Self-assembled monolayers (SAMS) and synthesis of planar micro- and nanostructures. *Journal of Macromolecular Science-Polymer Reviews* **2004,** *C44* (2), 175-206.
51. Bard, A. J.; Faulkner, L. R., *Electrochemical Methods Fundamentals and applications*. 2nd ed.; John Wiley & Sons: 2000.
52. Goes, M. S.; Rahman, H.; Ryall, J.; Davis, J. J.; Bueno, P. R., A Dielectric Model of Self-Assembled Monolayer Interfaces by Capacitive Spectroscopy. *Langmuir* **2012,** *28* (25), 9689-9699.
53. Lehr, J.; Weeks, J. R.; Santos, A.; Feliciano, G. T.; Nicholson, M. I. G.; Davis, J. J.; Bueno, P. R., Mapping the ionic fingerprints of molecular monolayers. *Physical Chemistry Chemical Physics* **2017,** *19* (23), 15098-15109.
54. Garrote, B. L.; Santos, A.; Bueno, P. R., Perspectives on and Precautions for the Uses of Electric Spectroscopic Methods in Label-free Biosensing Applications. *Acs Sensors* **2019,** *4* (9), 2216-2227.
55. Fernandes, F. C. B.; Andrade, J. R.; Bueno, P. R., A nanoscale redox-active composite as a low-fouling interface for capacitive assaying. *Sensors and Actuators B-Chemical* **2019,** *291*, 493-501.
56. Bisquert, J.; Garcia-Belmonte, G.; Bueno, P.; Longo, E.; Bulhoes, L. O. S., Impedance of constant phase element (CPE)-blocked diffusion in film electrodes. *Journal of Electroanalytical Chemistry* **1998,** *452* (2), 229-234.
57. Bisquert, J.; Garcia-Belmonte, G.; Fabregat-Santiago, F.; Bueno, P. R., Theoretical models for ac impedance of finite diffusion layers exhibiting low frequency dispersion. *Journal of Electroanalytical Chemistry* **1999,** *475* (2), 152-163.
58. Bueno, P. R., Nanoscale origins of super-capacitance phenomena. *Journal of Power Sources* **2019,** *414*, 420-434.
59. Oliveira, R. M. B.; Fernandes, F. C. B.; Bueno, P. R., Pseudocapacitance phenomena and applications in biosensing devices. *Electrochimica Acta* **2019,** *306*, 175-184.